JOURNAL OF MATERIALS SCIENCE 24 (1989) 2209–2213

Pressure derivatives of elastic constants of monoclinic $M(NO_3)_3 \cdot 9H_2O$ (M = Al, Fe, Cr) and third-order elastic constants of $Al(NO_3)_3 \cdot 9H_2O$

E. BEHNKE, S. HAUSSÜHL
Institut für Kristallographie der Universität zu Köln, Zülpicher Strasse 49, 5000 Köln 1, West Germany

The elastic constants and their pressure and temperature derivatives of monoclinic $M(NO_3)_3 \cdot 9H_2O$ (M = Al, Fe, Cr) have been determined from ultrasonic resonance frequencies of thick plates and from their temperature- and pressure-induced shifts. In addition, the complete third-order elasticity tensor of $Al(NO_3)_3 \cdot 9H_2O$ has been evaluated from a combination of measurements of shifts of ultrasonic resonance frequencies produced by hydrostatic pressure and uniaxial stresses in various directions. The elasticity tensors of the three isotypic salts and their temperature and pressure derivatives are almost identical. The elasticity tensor exhibits a distinct anisotropy as well as the tensor of thermal expansion. The thermoelastic constants behave quite normally, whereas the pressure derivatives show anomalous features, i.e. some of them are negative similar to the situation in cubic $Ba(NO_3)_2$ and α-ammonium or α-selenate alums. These effects are accompanied by a very small, even negative, thermal expansion. The third-order elastic constants of $Al(NO_3)_3 \cdot 9H_2O$ also reflect this anomalous behaviour.

1. Introduction

An earlier study of the pressure derivatives of elastic constants on the cubic nitrates $X(NO_3)_2$, X = Sr, Ba, Pb, revealed negative values dc_{11}/dp and dc_{12}/dp of $Ba(NO_3)_2$, whereas $Sr(NO_3)_2$ and $Pb(NO_3)_2$ did not show any anomaly of that type [1]. In the meantime, similar anomalies have been detected on ammonium and selenate alums of the α-type [2].

In the present paper we report comparable effects observed on monoclinic nitrates $M(NO_3)_3 \cdot 9H_2O$, M = Al, Fe, Cr (MNN). For the aluminium compound we also tried to determine the complete third-order elasticity tensor in order to decide which components of that tensor contribute substantially to the anomalous pressure dependence of the second-order elastic constants.

2. Experimental procedure

Single crystals of optical quality of the three compounds were grown from aqueous solutions by temperature-controlled cooling in the range 290 to 280 K. Standard-type equipment was employed. The growth rate was kept below 0.5 mm d^{-1}. After several generations of growth, single-crystalline specimens with dimensions up to 40 mm were obtained. The crystals exhibit a morphology compatible with the known point symmetry group 2/m. The following forms, ordered according to their morphological rank, are observed:

$$\{1\,1\,0\},\ \{0\,1\,1\},\ \{0\,0\,1\},\ \{1\,1\,1\},\ \{1\,0\,2\}.$$

The crystallographic reference system, introduced by Groth [5], for the aluminium salt ($a_1 : a_2 : a_3$ = 1.13 : 1 : 1.92, α_2 = 131°36′) was used. The corresponding X-ray metric data are shown in Table I. The axes, e_i, of the Cartesian reference system for the properties reported here were chosen as follows:

$$\boldsymbol{e}_2 \parallel \boldsymbol{a}_2,\ \boldsymbol{e}_3 \parallel \boldsymbol{a}_3,\ \boldsymbol{e}_1 = \boldsymbol{e}_2 x \boldsymbol{e}_3.$$

As a first step, the second-order elastic constants (SOEC), c_{ij}, and their temperature derivatives, $d \log c_{ij}/dT$, were determined at room temperature and zero pressure, from ultrasonic resonance frequencies and their variations induced by a change of temperature. The specimens were cut in the form of plane-parallel plates with dimensions of about 10 mm. The deviation from plane-parallelity on each pair of faces was kept below 1 μm. As the crystals are hygroscopic at normal humidity ($\sim 60\%$), the specimens were coated with a thin oil-film. For the detection of acoustic resonances, which are excited by X- and Y-cut quartz plates attached to the specimen, we used the diffraction of monochromatic laser light. During a slow-frequency sweep of the ultrasonic generator the resonances are easily recognized by sharp maxima of the intensity of the diffracted beam. Details of the method have been outlined earlier [6]. A total of 19 different acoustic modes propagating in directions $\boldsymbol{e}_i$ and $(\boldsymbol{e}_i \pm \boldsymbol{e}_j)$ were investigated. A manual-evaluation similar to that employed for the determination of the elasticity tensor of gypsum and other monoclinic crystals [7] yielded a first set of elastic constants. That procedure is based on the Christoffel equations

$$| - \delta_{ik} \varrho v^2 + c_{ijkl} g_j g_l | = 0 \qquad (1)$$

g_i are components of the unit vector pointing parallel to the propagation vector, c_{ijkl} components of the

0022–2461/89 $03.00 + .12

TABLE I X-ray metric data

	a_1 (nm)	a_2 (nm)	a_3 (nm)	α_2	Reference
Al	1.086	0.959	1.383	94°30′	[3]
Fe	1.103	0.970	1.399	95°30′	[4]
Cr	1.098	0.968	1.392	95°44′	[3]

elasticity tensor, ϱ the density, v the propagation velocity, and δ_{ik} the Kronecker symbol. A subsequent least-squares procedure involving all measurements yielded an improved set of elastic constants. The thermoelastic constants $T_{ij} = \mathrm{d} \log c_{ij}/\mathrm{d}T$ were obtained from the relation

$$T_{ij} \approx \frac{\Delta(\varrho v^2)}{\varrho v^2 \Delta T} \approx \frac{\Delta \varrho}{\varrho \Delta T} + \frac{2\Delta D}{D \Delta T} + \frac{2\Delta f}{f \Delta T} \qquad (2)$$

where $c_{ij} = \varrho v^2$ represents a certain combination of elastic constants. The right-hand side contains the variation of density, specimen thickness, D, along the propagation direction and resonance frequency, f, after a change of temperature, ΔT. The coefficients of thermal expansion were measured on large single crystals with the aid of an inductive gauge dilatometer in the range 250 to 300 K (see Table IV). The values thus obtained for c_{ij} and T_{ij}, including standard deviation, are listed in Table II.

In the second step we studied the variation of resonance frequencies of the acoustic modes of our specimens upon application of hydrostatic pressure, p, up to 1.5 kbar. The changes of ϱv^2 are given by

$$\frac{\Delta(\varrho v^2)}{\varrho v^2 \Delta p} \approx \frac{\Delta \varrho}{\varrho \Delta p} + \frac{2\Delta D}{D \Delta T} + \frac{2\Delta f}{f \Delta p} \qquad (3)$$

The first and second term on the right-hand side correspond to volume compressibility and linear compressibility which are both calculated from the known elastic constants [6]. The application of a least-squares procedure yielded the values $P_{ij} = \mathrm{d}c_{ij}/\mathrm{d}p$ given in Table II. Finally, we also measured the shifts of resonance frequencies induced by uniaxial stresses up to 30 bar cm^{-2} on the specimens of $Al(NO_3)_3 \cdot 9H_2O$. The details of the method employed have already been outlined in the case of alums [8] and orthorhombic calcium formate [9]. The basic equations combining the observable quantities with the unknown third-order elastic constants (TOEC) are

$$\frac{\partial(\varrho W^2)}{\partial \sigma_{pq}} = k_p k_q + 2\varrho W^2 s^{\mathrm{T}}_{ijpq} w_i w_j + c_{ijklmn} k_j k_l w_i w_k \qquad (4)$$

All quantities are taken at zero stress. W is the "natural velocity" of a sound wave defined by $W = (l_0/l_1)v$, where l_0 and l_1 denote the length of the specimen in the direction of the propagation vector without and with external stresses, respectively, v is the measured wave velocity of plane elastic waves, ϱ the density. σ_{ij}, s^{T}_{ijkl}, k_i and w_i are the components of the isothermal static stress tensor, the elasticity s-tensor (inverse c-tensor), the components of the propagation vector and the displacement vector, respectively. The TOEC are defined as

$$c_{ijklmn} = \varrho \frac{\partial^3 U}{\partial \eta_{ij} \partial \eta_{kl} \partial \eta_{mn}} \qquad (5)$$

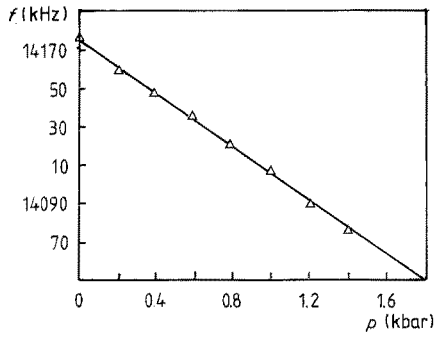

Figure 1 Frequency shift versus hydrostatic pressure observed on the longitudinal wave propagation along direction {0 1 0}.

where U is the internal energy per unit mass and η_{ij} are the components of the Lagrangian deformation tensor.

The relation between measured quantities $\partial f/\partial \sigma_{pq}$ and the left-hand side of the basic equation is

$$\frac{\partial(\varrho W^2)}{\partial \sigma_{pq}} = 2\varrho W^2 \frac{\partial f}{f \partial \sigma_{pq}} \qquad (6)$$

where f is the relevant resonance frequency as above [10].

In all cases we obtained a linear dependency of the shift of resonance frequencies on hydrostatic and uniaxial pressure. Examples are shown in Figs 1 and 2. A list of the equations combining the experimental values and the expressions of the third-order elastic constants involved can be obtained from the authors. Finally, a total of 102 different arrangements of hydrostatic and uniaxial pressure with different propagation vectors and modes were investigated. The strongly overdetermined system of equations for the 32 independent third-order elastic constants in crystals of point symmetry 2/m was again solved by a least-squares procedure. The values obtained including standard deviation are presented in Table III.

In order to obtain an impression of the temperature variation of the third-order elastic constants, we also determined the slope of the resonance-frequency against temperature curve for all 102 arrangements in the range between 293 and 273 K. A least-squares evaluation of these measurements yielded the values $\partial c_{ijk}/\partial T$ given in Table III. Owing to the very small effects they should be considered as of only qualitative character.

3. Discussion

3.1. General behaviour (SOEC)

The three isotypic compounds exhibit a quite similar

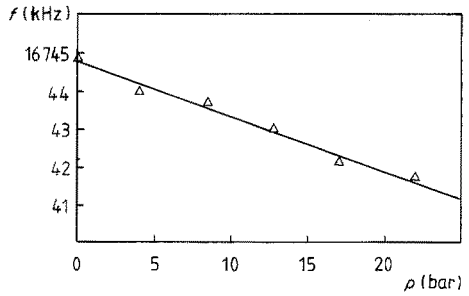

Figure 2 Frequency shift versus uniaxial pressure parallel to $\mathbf{e}_2$, observed on the longitudinal wave propagating along direction {0 1 0}.

TABLE II Elastic constants, c_{ij}, pressure derivatives, P_{ij} dc_{ij}/dp, and temperature derivatives, T_{ij} $d \log c_{ij}/dT$ ($10^{-3} K^{-1}$) of $M(NO_3)_3 \cdot 9H_2O$, M = Al, Cr, Fe

	ij												
	11	22	33	44	55	66	12	13	23	15	25	35	46
$Al(NO_3)_3 \cdot 9H_2O$													
c_{ij} (GPa)	39.03 ± 0.42	20.71 ± 0.08	39.60 ± 0.48	7.99 ± 0.04	8.96 ± 0.12	6.51 ± 0.03	14.82 ± 0.22	17.39 ± 0.23	15.88 ± 0.23	−4.39 ± 0.03	−2.14 ± 0.03	−0.85 ± 0.02	0.41 ± 0.02
P_{ij}	9.10 ± 0.04	−1.71 ± 0.01	−0.72 ± 0.03	1.31 ± 0.05	−0.91 ± 0.03	−3.59 ± 0.01	−0.79 ± 0.06	5.65 ± 0.07	−2.72 ± 0.01	0.24 ± 0.01	−9.64 ± 0.18	4.19 ± 0.08	1.01 ± 0.02
T_{ij}	−0.87 ± 0.02	−0.79 ± 0.02	−0.97 ± 0.03	−1.31 ± 0.02	−1.27 ± 0.03	−1.16 ± 0.02	−0.62 ± 0.02	−0.34 ± 0.01	0.11 ± 0.03	0.12 ± 0.01	−10.78 ± 0.38	−0.66 ± 0.04	−7.07 ± 0.20
$Cr(NO_3)_3 \cdot 9H_2O$													
c_{ij} (GPa)	40.15 ± 0.45	21.30 ± 0.09	40.96 ± 0.47	8.18 ± 0.05	9.23 ± 0.14	6.68 ± 0.04	15.25 ± 0.24	17.90 ± 0.22	16.34 ± 0.23	−4.16 ± 0.03	−2.05 ± 0.03	−0.81 ± 0.02	0.43 ± 0.01
P_{ij}	9.36 ± 0.04	−1.66 ± 0.02	−0.68 ± 0.03	1.35 ± 0.04	−0.89 ± 0.05	−3.47 ± 0.03	−0.74 ± 0.08	5.81 ± 0.05	−2.80 ± 0.01	0.22 ± 0.02	−9.92 ± 0.23	4.07 ± 0.06	0.97 ± 0.05
T_{ij}	−0.85 ± 0.02	−0.81 ± 0.03	−0.94 ± 0.03	−1.27 ± 0.03	−1.24 ± 0.02	−1.19 ± 0.03	−0.59 ± 0.03	−0.34 ± 0.01	0.12 ± 0.03	0.09 ± 0.02	−10.30 ± 0.34	−0.62 ± 0.03	−7.27 ± 0.16
$Fe(NO_3)_3 \cdot 9H_2O$													
c_{ij} (GPa)	40.46 ± 0.46	21.47 ± 0.10	41.55 ± 0.46	8.28 ± 0.04	9.30 ± 0.14	6.75 ± 0.04	15.37 ± 0.25	18.03 ± 0.23	16.46 ± 0.24	−4.11 ± 0.02	−1.97 ± 0.03	−0.72 ± 0.01	0.43 ± 0.01
P_{ij}	9.44 ± 0.04	−1.63 ± 0.03	−0.69 ± 0.03	1.39 ± 0.03	0.88 ± 0.05	−3.43 ± 0.04	−0.76 ± 0.06	5.86 ± 0.05	−2.84 ± 0.02	0.25 ± 0.02	−9.99 ± 0.21	4.05 ± 0.05	0.94 ± 0.05
T_{ij}	−0.84 ± 0.02	−0.81 ± 0.03	−1.00 ± 0.03	−1.22 ± 0.02	−1.18 ± 0.02	−1.21 ± 0.03	−0.60 ± 0.03	−0.29 ± 0.02	0.23 ± 0.03	−0.02 ± 0.01	−9.92 ± 0.31	−0.57 ± 0.02	−6.91 ± 0.15

TABLE III Third-order elastic constants, c_{ijk}, and temperature derivatives of third-order elastic constants, dc_{ijk}/dT, of $Al(NO_3)_3 \cdot 9H_2O$

ijk	c_{ijk} (GPa)	$\frac{dc_{ijk}}{dT}$ (GPa K^{-1})	ijk	c_{ijk} (GPa)	$\frac{dc_{ijk}}{dT}$ (GPa K^{-1})
111	−11.18 ± 0.56	0.42 ± 0.07	233	−4.66 ± 0.71	0.46 ± 0.02
112	−4.99 ± 0.23	0.53 ± 0.08	235	4.04 ± 0.69	−0.15 ± 0.03
113	−17.32 ± 0.65	0.09 ± 0.01	244	−4.10 ± 0.73	−0.02 ± 0.01
115	−36.57 ± 1.27	−1.68 ± 0.13	246	−2.39 ± 0.68	−0.18 ± 0.02
122	15.37 ± 0.81	0.17 ± 0.03	255	−17.96 ± 0.65	−0.09 ± 0.01
123	15.19 ± 0.83	−0.15 ± 0.02	266	−5.58 ± 0.43	0.06 ± 0.01
125	−2.35 ± 0.93	0.36 ± 0.03	333	−0.56 ± 0.31	0.74 ± 0.03
133	14.32 ± 0.59	0.72 ± 0.04	335	39.86 ± 1.45	−0.13 ± 0.02
135	−13.85 ± 0.62	−0.29 ± 0.03	344	1.17 ± 0.53	−0.13 ± 0.02
144	−7.90 ± 0.64	0.05 ± 0.01	346	−19.99 ± 0.88	0.23 ± 0.03
146	−9.77 ± 0.92	−0.21 ± 0.04	355	−12.23 ± 0.65	0.04 ± 0.01
155	−22.19 ± 1.02	0.36 ± 0.03	366	−28.76 ± 1.78	0.20 ± 0.02
166	−1.78 ± 0.76	−0.16 ± 0.01	445	2.38 ± 0.78	0.03 ± 0.01
222	3.37 ± 1.34	−0.07 ± 0.01	456	4.64 ± 0.75	−0.05 ± 0.01
223	17.14 ± 0.89	−0.16 ± 0.02	555	39.74 ± 1.87	0.32 ± 0.03
225	−2.87 ± 0.99	0.35 ± 0.03	556	−21.95 ± 1.31	0.16 ± 0.02

physical behaviour in respect to all properties reported here, as expected. Apparently, the preponderance of the $(NO_3)_3 \cdot 9H_2O$ framework suppresses the influence of the different trivalent cations.

Only very slight differences exist in the metric data and morphology. The most impressive differences are observed with the optical absorption (aluminium salt, fully transparent; chromium salt, deep red-violet; iron salt, faintly violet). A similar situation is found in the alums of aluminium, chromium and iron [11]. The crystals reflect their low symmetry in a strong anisotropy of thermal expansion and elastic properties. In direction $(\boldsymbol{e}_1 + \boldsymbol{e}_3)$ a surprising negative thermal expansion is observed (see Table IV; values in the principal axes system). The elastic anisotropy is best characterized by $c_{11} \sim c_{33} \sim 2c_{22}$. As expected from the Grüneisen relation, the directions $\boldsymbol{e}'_1$ of maximum and minimum thermal expansion nearly coincide with the directions of minimum and maximum longitudinal elastic resistance

$$c'_{11} = c'_{1111} = u_{1i}u_{1j}u_{1k}u_{1l}c_{ijkl} \qquad (7)$$

u_{1i} are the direction cosines of $\boldsymbol{e}'_1$. c'_{11} possess extrema values in the directions $\boldsymbol{e}'_1 = 0.88\boldsymbol{e}_1 - 0.46\boldsymbol{e}_3$ (max) and $\boldsymbol{e}'_1 = -0.57\boldsymbol{e}_1 - 0.81\boldsymbol{e}_3$ (min). The difference beween these two values, however, is relatively small in comparison to the huge anisotropy of the thermal expansion.

The thermoelastic constants, T_{ij}, exhibit only a small anisotropy.

3.2. Pressure derivatives of the elastic constants

The most surprising result of the present study is the existence of negative pressure derivatives of certain elastic constants in MNN, like P_{22}, P_{33}, P_{55}, P_{66}, P_{12}, P_{23} and P_{25}. Further, the derivative P_{11} is positive, in absolute magnitude about ten times larger than P_{22} or P_{33}, a quite unusual anisotropy. The maximum value of $P'_{11} = dc'_{11}/dp$ is observed in direction $\boldsymbol{e}'_1 = 0.79\boldsymbol{e}_1 - 0.42\boldsymbol{e}_3$, the minimum in direction $\boldsymbol{e}'_1 = -0.44\boldsymbol{e}_1 - 0.79\boldsymbol{e}_3$. These directions almost coincide with the extrema of the longitudinal elastic resistance c'_{11} and the linear thermal expansion discussed above. The general anomalous pressure dependence may be expressed by the quantity dK^{-1}/dp, where K is the volume compressibility. In stable crystals so far investigated, $dK^{-1}/dp \sim 5$. Here we find a value as low as -1.5, indicating a quite anomalous behaviour.

Crystals which exhibit similar anomalies in respect to P_{ij} are $Ba(NO_3)_2$ [1, 12] and certain α-alums [2]. Other examples are found only in cases of a phase transition, e.g. $Li_2Ge_7O_{15}$ [13]. Thorough investigations on other nitrates like $Sr(NO_3)_2$, $Pb(NO_3)_2$, $NaNO_3$ and $AgNO_3$ [12, 14] did not yield further examples of negative P_{ij}. The situation with the alums is different from that in the MNN group and $Ba(NO_3)_2$, because the alums exhibit nonlinear effects with curved $c_{ij}(p)$ curves, indicating strong values of $\partial^2 c_{ij}/\partial p^2$. Such a behaviour is not observed in our crystals under investigation. However, in common, all these crystals with negative P_{ij} possess a very small thermal expansion compared with other crystals of similar structure.

As all attempts to interpret the anomalies in $Ba(NO_3)_2$, which possesses a simple structure related to the CaF_2-type, were hitherto not successful, we are not surprised that analogous efforts on the structurally highly complicated MNN group did not lead even to a qualitative explanation of the anomalies. However, it should be emphasized that the peculiar properties of the MNN group underline once more

TABLE IV Coefficients of thermal expansion, α_{ij}, of $M(NO_3)_3 \cdot 9H_2O$, M = Al, Fe, Cr (10^{-6} K^{-1}). α'_{ii} values in the principal axes $\boldsymbol{e}'_1$ and $\boldsymbol{e}'_3$

	α_{11}	$\alpha_{22} = \alpha'_{22}$	α_{33}	α_{13}	α'_{11}	α'_{33}	$\boldsymbol{e}_1$	$\boldsymbol{e}'_3$
$Al(NO_3)_3 \cdot 9H_2O$	24.6(5)	27.9(5)	15.3(4)	−121.8(20)	136.6(6)	−98.2(1)	(0.7, 0, 0.7)	(0.7, 0, 0.7)
$Fe(NO_3)_3 \cdot 9H_2O$	32.2(5)	39.2(8)	7.5(2)	−104.5(20)	125.4(3)	−85.1(1)	(0.8, 0, 0.7)	(0.7, 0, 0.8)
$Cr(NO_3)_3 \cdot 9H_2O$	38.1(7)	44.8(9)	10.8(3)	−93.6(16)	119.0(1)	−70.2(2)	(0.8, 0, 0.7)	(0.7, 0, 0.8)

that simple rules used for the prediction of properties of solid materials like those recently discussed by Yamamoto and Anderson [15] should be considered as unreliable, at least as a generally valid approach.

3.3. Third-order elastic constants of $Al(NO_3)_3 \cdot 9H_2O$

The TOEC of $Al(NO_3)_3 \cdot 9H_2O$ express the deviations from Hooke's law. In most crystals investigated so far we observe negative tensor components c_{ijklmn}, i.e. the response to an external uniaxial pressure is an increase in the elastic constants. As in the case of the c_{ij} we also expect that the TOEC will possess a magnitude comparable to that in alums. This is true; however, we also observed positive TOEC in $Al(NO_3)_3 \cdot 9H_2O$ in accordance with negative P_{ij} discussed in Section 2. Using Voigt's notation these are:

$$c_{122},\ c_{123},\ c_{133},\ c_{222},\ c_{223},\ c_{235},\ c_{335},\ c_{344},\ c_{445},\ c_{456},\ c_{555}.$$

Due to the experimental difficulties, which stem from the necessary limitation of applied uniaxial stresses, the probable errors of the TOEC are considerably larger than those of the c_{ij}. However, positive values for c_{122}, c_{123}, c_{223}, c_{335} and c_{555} are out of the question.

A rotation of the Cartesian system around the e_2-axis by $+27.9°$ gives the new e_1-axis an orientation parallel to the direction of maximum longitudinal elastic constant, c'_{11}. In this system the anisotropy of the TOEC is still more clearly expressed ($\sim 10\%$).

Further studies on other nitrates and related compounds like borates and carbonates are desirable in order to elucidate the origin of the anomalies reported here.

References

1. D. GERLICH, M. WOLF and S. HAUSSÜHL, *J. Phys. Chem. Solids* **B9** (1978) 1089.
2. S. HAUSSÜHL, A. KRANZMANN and R. PODESWA, *J. Mater. Sci. Lett.* **6** (1987) 423.
3. K. K. KANNAN and M. A. VISAWAMITRA, *Acta Crystallogr.* **19** (1965) 151.
4. N. J. HAIR and J. K. BEATTICE, *Inorg. Chem.* **16** (1977) 245.
5. P. GROTH, *Chem. Krystallogr.* **2** (1908) 133.
6. S. HAUSSÜHL, "Kristallphysik" (Weinheim, Leipzig, 1983).
7. *Idem, Z. Krist.* **122** (1965) 311.
8. S. HAUSSÜHL and P. PREU, *Acta Crystallogr.* **A34** (1978) 442.
9. S. HAUSSÜHL and W. CHMIELEWSKY, *ibid.* **A37** (1981) 361.
10. D. C. WALLACE, *Solid State Phys.* **25** (1970) 301.
11. S. HAUSSÜHL, *Z. Krist.* **116** (1961) 371.
12. TH. NARZ, Diplomarbeit, Köln (1985).
13. S. HAUSSÜHL, *Solid State Commun.* **46** (1983) 423.
14. S. HAUSSÜHL, *Z. Krist.* (1989) to be published.
15. S. YAMAMOTO and O. L. ANDERSON, *Phys. Chem. Mineral* **14** (1987) 332.

Received 2 October 1987
and accepted 26 January 1988